Trad. Med. J., September-December 2022
Vol. 27(3), p 218-230
ISSN-p : 1410-5918 ISSN-e : 2406-9086

Submitted : 29-08-2022
Revised : 20-10-2022
Accepted : 28-11-2022

Antifungal Activities of Phytochemicals from *Annona muricate* (Sour Sop): Molecular Docking and Chemoinformatics Approach

Misbaudeen Abdul-Hammed[1*], Ibrahim Adedotun Olaide[1], Hadijat Motunrayo Adegoke[1,2], Monsurat Olajide[1,3], Oluwasegun Johnson Osilade[1], Tolulope Irapada Afolabi[1], Adelayo Idayat Abdul-Hammed[1,4]

[1] Computational and Biophysical Chemistry Unit, Department of Pure and Applied Chemistry, Ladoke Akintola University of Technology, LAUTECH, Ogbomoso, Oyo State, Nigeria
[2] Genomics Unit, Helix Biogen Institute, Ogbomoso, Oyo State, Nigeria
[3] Department of Chemical Sciences, Crescent University, Abeokuta, Ogun State, Nigeria
[4] Department of Computer Science, Ladoke Akintola University of Technology, LAUTECH, Ogbomoso, Oyo State, Nigeria

ABSTRACT

Fungal infection has become a persistent problem in humans and is sometimes life-threatening in immune-compromised individuals. This work aims to study phytochemicals from *Annona muricata* (sour sop) as probable antifungal agents against *Candida albicans* sterol 14α-demethylase target receptor by Computer Aided-Drug Design (CADD) approach using voriconazole and fluconazole as standard drugs. A modern method of drug discovery by molecular docking and chemoinformatics was used to screen 131 isolated phytochemicals with medicinal properties from *Annona muricata* against *Candida albicans* 'sterol 14α-demethylase, a prominent target receptor for most anti-fungal drugs, towards the development of new anti-fungal therapeutic agents and a new approach to treat patients with fungal infections. The compounds were all subjected to analyses like ADMET, drug-likeness, bioactivity, oral-bioavailability and PASS. The results of the docking simulation and chemoinformatics analyses showed that muricin M (-7.9 kcal/mol), chlorogenic acid (-8.2 kcal/mol), roseoside (-8.5 kcal/mol) and caffeoylquinic acid (-8.1 kcal/mol) are potential drug candidates for treating fungal infections due to their excellent properties such as binding affinities, ADMET profile, drug-likeness, bioactivity, binding mode and interactions with the target receptor. Thus, muricin M, chlorogenic acid, roseoside and caffeoylquinic acid are recommended for further analyses towards the development of further antifungal drugs.

Keywords: Chemoinformatics, Phytochemicals, *Annona muricata*, Fungal infection, *Candida albicans*.

INTRODUCTION

Fungal infections affect a wide diversity of populations and are caused by many different fungal pathogens from various sources (Bongomin et al., 2017). Many medical specialists come across patients with fungal infections, including general practitioners like paediatricians, dermatologists, ophthalmologists, oncologists, haematologists, intensive-care-unit practitioners, internal medicine and AIDS physicians, and otolaryngologists, which complicate the provision of holistic education about fungal infections (Tudela and Denning, 2017). The rate of mortality due to fungal infections and illnesses is currently at its peak. Severe fungal infections often arise because of other health issues, including acquired immunodeficiency syndrome (AIDS), cancer, asthma, diabetes, organ transplantation, and treatment with corticosteroids (Al Aboody and Mickymaray, 2020). There are different types of fungal diseases such as fungal nail infections, vaginal candidiasis, ringworm, and so on. Some serious and life-threatening fungal diseases such as aspergillosis, Candida auris infection, and invasive candidiasis (Kohler et al., 2015) also affect humans with a weakened immune system (patients with HIV, cancer, organ transplants, or certain medications) (Al Aboody and Mickymaray, 2020).

In an attempt to treat fungal illnesses, four groups of antifungal medications are frequently available to treat fungal infections such as azoles (clotrimazole, fluconazole, itraconazole, ketoconazole, miconazole voriconazole, posaconazole, ravuconazole), echinocandins (caspofungin, micafungin, and anidulafungin), flucytosine (5-fluorocytosine) and polyenes (pimaricin, trichomycin, candicidin, amphotericin B, nystatin, methyl partricin) (Al Aboody and Mickymaray, 2020). Although, the global issue of antibiotic resistance does not exclude fungus infection. Current antifungal drugs are imperfect, and new approaches are vital including those that support patients-host defences (Tudela and

***Corresponding author : Misbaudeen Abdul-Hammed**
Email : mabdul-hammed@lautech.edu.ng

Denning, 2017). Sterol 14α-demethylase (CYP51, P45014DM, Erg11) is a member of the cytochrome P450 superfamily, which catalyzes the oxidative removal of the 14α-methyl group (C-32) of lanosterol to give 14, 15-desaturated intermediates in ergosterol biosynthesis (Sheng *et al.,* 2009). C*andida albicans* CYP51 consists of 528 amino acids (62kDa), including the 48-amino acid-long N-terminal membrane anchor sequence (Hargrove *et al.,* 2017).

Over the past century, the phytochemicals in plants have been a channel for pharmaceutical discovery (Moghadamtousi et al., 2015). Natural products from plants have been used to help sustain the health of mankind since the dawn of medicine. The importance of the active ingredients of plants in agriculture and medicine has stimulated significant scientific interest in the biological activities of these substances due to the increasing failure of chemotherapeutic agents, and antibiotic resistance exhibited by pathogenic organisms (Moghadamtousi et al., 2015). Researchers are increasingly turning their attention to traditional medicine, screening several medicinal plants for their potential antimicrobial activities for new leads to develop a better drug against microbial infections (Moghadamtousi et al., 2015). Plants with a lengthy account of ethnomedical usage are regarded as abundant sources of vital phytoconstituents that offer therapeutic or health advantages against a variety of illnesses and diseases. Annona muricata (Soursop) is not left out among the plants with great traditional importance (Moghadamtousi et al., 2015). It was reported that Annona *muricata* contains varieties of bioactive compounds and has a very potent antimicrobial ability that can be associated with rich phytoconstituents like phenols, flavonoids, alkaloids, and acetogenins among others. All parts of *Annona muricata* including bark, leaves, roots, and fruits are used in natural medicine (Agu and Okolie, 2017).

The use of computational chemistry in drug design and discovery cannot be over-emphasized. Various studies have reported the efficacy of the computational approach in proposing potential drug leads in different phytochemicals against various diseases including coronavirus (Aanouz *et al.,* 2020; Abdul-Hammed *et al.,* 2021; Falade *et al.,* 2021), breast cancer (Abdul-Hammed *et al.,* 2022), Alzheimer's diseases among others with higher success rates. The method is quite efficient and cost-effective in the identification of potential lead compounds in drug development. In the quest to propose a promising treatment for fungi infections with the aid of natural products, this study demonstrated the inhibitory potentials of 131 phytochemicals from *Annona muricata* against *Candida albicans* serol 14α-demethylase (PDB ID: 5TZ1) target receptor by using the Computer Aided-Drug Design (CADD) approach.

METHODOLOGY

Material

The software used are PyRx virtual screening tool, BIOVIA Discovery studio visualizer, Pymol, CASTp and Spartan' 14.

Methods

Preparation of the Ligands

One hundred and thirty-one (131) isolated phytochemicals (ligands) from *Annona muricata* and two standard drugs (fluconazole and voriconazole) were used for this research. The two-dimensional structures of all the ligands and standards were retrieved from the PubChem database (https://pubchem.ncbi.nlm.nih.gov) and converted to 3D structures using Spartan' 14 software. To obtain ligands and standards with the most stable conformation for docking simulation, a conformer search was carried out using Conformer Distribution (Molecular Mechanics/ MMFF) set on Spartan'14 software. The most stable conformers obtained were optimized using the density functional theory method (DFT) at B3LYP and 6-31G* basis set, to have structures with the best equilibrium geometry before molecular docking simulations.

Preparation of the Target Receptor

The 3D crystal structure of Sterol 14α-demethylase in complex with CYP51 inhibitor (PDB ID: 5TZ1) (Figure 1) was retrieved from Protein Data Bank (PDB) (*www.rcsb.org*) with a resolution of 2.00 Å (Hargrove *et al.,* 2017), recommended for a protein of excellent quality for molecular docking. The protein was prepared by removing water molecules, ligands, and other heteroatom residues present in the structure to avoid unwanted interactions and interference with the active site, and the Ramachandran Plot (Figure 2) of the protein was obtained using Discovery Studio Software 2019. The binding pocket of the initial inhibitors present in 5TZ1 was used in determining the binding parameters as -28.96, 33.22, and 33.22 for x, y, and z respectively using the grid box of the inhibitor complexed with the target receptor.

Identification and Validation of the Active Sites

Computed Atlas for Surface Topography of Proteins (CASTp), (http://sts.bioe.uic.edu/castp/index.html?2011) (Tian *et al.,* 2018), and Biovia

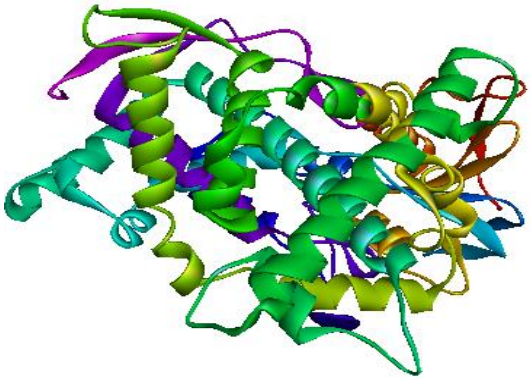

Figure 1. Crystal structure of Sterol 14α-demethylase (PDB 1D: 5TZ1). The alpha helices, beta sheets, and amino acid chain turns are in magenta, yellow and pale blue colours, respectively, while all other amino acid residues are coloured white.

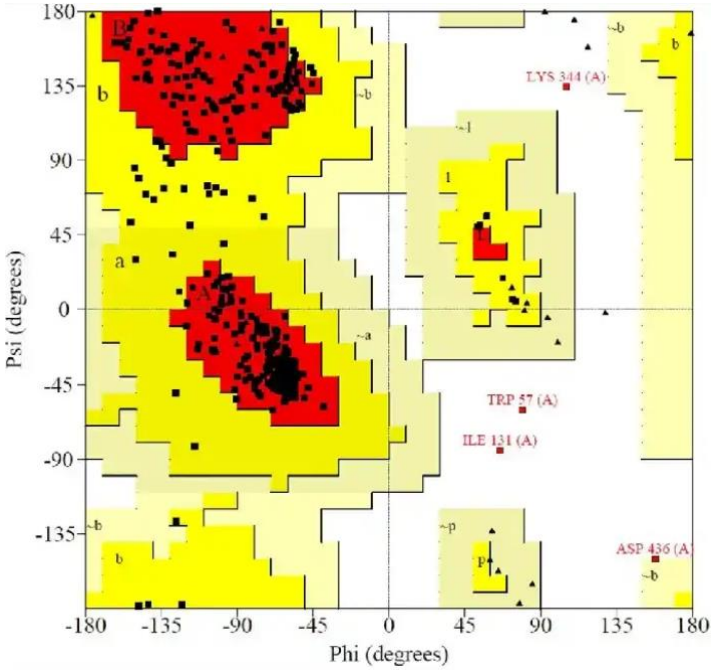

Figure 2. The Ramachandran plot of Sterol 14α-demethylase (PDB: 5TZ1) from VADAR (Volume, Area, and Dihedral Angle Reporter) web server. The colour codes in the plot correspond to conformations where atoms in the polypeptide come closer than the sum of their van der Waals radii which is sterically disallowed (white), regions where there are no steric clashes (red) and the allowed regions with alpha-helical and beta-sheet conformations (yellow).

Discovery Studio (2019) was used to determine the binding pocket, amino acids and all the ligand interactions in the active site of 5TZ1 receptor. Result obtained was then validated with the source journal of the protease from the protein data bank (www.rcsb.org) (Hargrove, et al. 2017).

Molecular Docking

The most stable optimized ligands and standards were docked with the target receptor using PyRx virtual screening software in duplicate (Dallakyan and Olson, 2015). The mean average binding affinities and standard deviation were

obtained. The binding affinities obtained were used to calculate the inhibition constant (Ki) of the docked ligands and standards against the target receptor as shown in the equations below.

$\Delta G = -RT \ln Ki$ ..... (1)

$Ki = \exp(-\Delta G/RT)$ ..... (2)

where R = Gas constant (1.987 × 10-3 kcal/mol), T = 298.15 K (absolute temperature); Ki = Inhibition constant, ΔG = Binding energy.

The docking results were viewed and analyzed using Biovia Drug discovery studio 2019 and PyMol software.

ADMET and Drug-Likeness Studies

The pharmacokinetic properties (absorption, distribution, metabolism, excretion, and toxicity, ADMET) of the ligands were predicted utilizing the admetSAR2 database (http://lmmd.ecust.edu.cn/admetsar2/) while drug-likeness prediction of ligands was carried out by Lipinski filter using molecular inspiration server (https://www.molinspiration.com/) (Dain a *et al.,* 2017).

Prediction of Activity Spectra for Substances (PASS) and Oral Bioavailability Assessment

The biological activities of the ligands from *Annona muricata* were analyzed for their antifungal property using the PASS software, (http://pharmexpert.ru/passonline/) while other properties related to the oral bioavailability properties of the ligands were obtained from the Swiss-ADME web tool (http://www.swissadme.ch/).

RESULT AND DISCUSSION

Structural and active site analysis of sterol 14α-Demethylase (PDB ID: 5TZ1)

The active sites of sterol 14α-Demethylase *(*PDB ID: 5TZ1) are located at the heme loop that contains the following residues: Tyr-64 Tyr-118 Leu-121 Thr-122 Phe-126 Ile-131 Tyr-132 Phe-228 Pro-230 Phe-233 Gly-303 Ile-304 Gly-307 Gly-308 Thr-311 Leu-376 His-377, H-bond Ser-378 Phe-380 Tyr-505 Ser-507 Met-508 (Hargrove *et al.,* 2017).

Molecular Docking Analysis

Molecular docking has shown great advancement in the predictions of therapeutic interventions by predicting bound conformations and free energies of binding for small-molecule ligands to macromolecular targets (protein) (El-Hachem *et al.,* 2017). It is used in the evaluation of the binding mode of inhibitors and receptors to guide the optimization of lead compounds (Dong *et al.,* 2019). The rule of thumb is "the higher the binding affinity, the lower the inhibition constant", and vice-versa (Ferreira *et al.,* 2015). The 131 ligands from *Annona Muricata* docked against sterol 14α-demethylase receptor using PyRx virtual screening tool include eighty-three (83) acetogenins, fourteen (14) alkaloids, three (3) cyclopeptides, ten (10) flavonoid triglycosides, thirteen (13) megastigmanes and eight (8) phenolics.

The docking scores and inhibition constants are shown in Table I. The binding affinities of the acetogenins range from -8.3 to -6.6 kcal/mol, with muricin L and muridienin 4 having the highest and lowest values, respectively. Thirty-one of the acetogenins have better inhibitory activities than the standard voriconazole (SD1) and fluconazole (SD2). The binding affinities of the alkaloids range from -8.9 to -7.5 kcal/mol, with anonaine and atherospemine having the highest and the lowest values respectively (Table I). Twelve alkaloids have better inhibitory activities than SD1 and SD2. The binding affinities of the cyclopeptides range from -11.5 to -6.6 kcal/mol, with annomuricatin C and annomuricatin B having the highest and the lowest values respectively. Two cyclopeptides have better inhibitory activities than SD1 and SD2. Flavonoid triglycosides have binding affinities ranging from -9.4 to -5.7 kcal/mol, with kaempferol-3-0-rutinoside and gallic acid having the highest and the lowest values, respectively, while nine of the flavonoid triglycosides have better inhibitory activities than SD1 and SD2. Also, the binding affinities of the docked megastigmanes and the phenolics range from -9.3 to -6.1 kcal/mol, and -9.8 to -6.1 kcal/mol, respectively with kaempferol-3-0-rutinoside and anoinol C having the highest and the lowest values, respectively for the megastigmanes, and kaempferol-3-0-rutinoside and anoinol C for the phenolics. In each case, five of the docked ligands have better inhibitory activities than SD1 and SD2. However, binding affinity is not enough to validate the reliability of the ligand as a potential drug candidate against the studied fungal infection. Therefore, all the ligands were subjected to other chemoinformatics analyses and toxicity tests.

Assessment of the ADMET Analysis

Absorption, distribution, metabolism, excretion, and toxicity (ADMET) prediction can guide the selection and optimization of lead compounds in the early stage of drug development. In the parameter settings, the aqueous solubility, blood-brain barrier penetration, hepatotoxicity, human intestinal absorption (HIA), and plasma protein binding were derived from the ADMETSAR2 web server (Dong *et al.,* 2019).

Table Ia. Ligands from *Annona muricata* and Standard drugs showing docking scores and the Inhibition Constants of the Interaction of Ligands with the Crystal structure of Sterol 14 α-demethylase (PDB ID: 5TZ1)

Ligands	Binding Affinity (ΔG), kcal/mol	Inhibition constants (K_i), μM	Ligands	Binding Affinity (ΔG), Kcal/Mol	Inhibition constants (K_i), μM
Acetogenins					
Muricin L	-8.3±0.07	0.65	Muricin B	-7.7±0.28	1.83
Annocatacin A	-8.1±0.49	0.92	Muricin H	-7.7±0.28	1.83
Arianacin	-8.0±0.00	1.09	Xylomaticin	-7.7±0.42	1.83
Cis-annonacin-10-One	-8.0±0.00	1.09	Muricapentocin	-7.7±0.35	1.83
Gigantetronenin	-8.0±0.28	1.09	Muricin A	-7.7±0.35	1.83
Muricin G	-8.0±0.28	1.09	Muricin D	-7.7±0.49	1.83
Muricin E	-8.0±0.07	1.09	Muricin I	-7.7±0.35	1.83
Annonacin	-7.9±0.07	1.30	Annomuricin C	-7.6±0.14	2.17
Annopentocin A	-7.9±0.21	1.30	Annonacin A	-7.6±0.28	2.17
Muricin M	-7.9±0.00	1.30	Annoreticuin-9-One	-7.6±0.57	2.17
Goniothalamicin	-7.9±0.21	1.30	Cis-Corrosolone	-7.6±0.14	2.17
Muricatocin C	-7.9±0.07	1.30	Cis-Uvariamicin	-7.6±0.42	2.17
Annocatalin	-7.8±0.21	1.54	Longifolicin	-7.6±0.07	2.17
Annomontacin	-7.8±0.00	1.54	Annomutacin	-7.5±0.28	2.58
Annomuricin A	-7.8±0.35	1.54	Cis-Panatellin	-7.5±0.21	2.58
Cis-Annomontacin	-7.8±0.21	1.54	Corossolin	-7.5±0.57	2.58
Corepoxylone	-7.8±0.28	1.54	Corossolone	-7.5±0.21	2.58
Javoricin	-7.8±0.21	1.54	Muricin J	-7.5±0.57	2.58
Annonancin-10-One	-7.7±0.14	1.83	Annomuricin B	-7.5±0.07	2.58
Annopentocin B	-7.7±0.35	1.83	Gigantetrocin B	-7.5±0.35	2.58
Cis-goniothalamicin	-7.7±0.14	1.83	Isoannonacinone	-7.5±0.35	2.58
Cis-reticulatacin-10-one	-7.7±0.78	1.83	Annomuricin E	-7.4±0.14	3.06
Cis-solamin	-7.7±0.21	1.83	Muricahexocin A	-7.4±0.42	3.06
Cis-Uvariamicin 1	-7.7±0.00	1.83	Muricatocin B	-7.4±0.14	3.06
Acetogenins (Cont'd)					
Muricin K	-7.4±0.57	3.06	Murihexocin B	-7.4±0.07	3.06
Murihexocin A	-7.4±0.14	3.06	Cis-Annonacin	-7.3±0.14	3.63
Murisolin	-7.4±0.28	3.06	Cohibin D	-7.3±0.42	3.63
Muricatetrocin A	-7.4±0.21	3.06	Epomuricenin A	-7.3±0.00	3.63
Muricatetrocin B	-7.4±0.35	3.06	Epomusenin B	-7.3±0.28	3.63
Muricatocin A	-7.4±0.49	3.06	Isoannonacin	-7.3±0.14	3.63
Muricin C	-7.4±0.07	3.06	Muricin N	-7.3±0.07	3.63
Alkaloids					
Anonaine	-8.9±0.00	0.23	(R)-4-O-methyl coclaurine	-8.1±0.07	1.00
Isolaureline	-8.6±0.00	0.39	Nornuciferine	-8.0±0.00	1.09
Coreximine	-8.5±0.00	0.46	Reticuline	-8.0±0.00	1.09
Xylopine	-8.4±0.00	0.55	Stepharine	-7.9±0.00	1.30
Anomuricine	-8.2±0.00	0.77	Asimilobine	-7.7±0.00	1.83
Anomurine	-8.2±0.00	0.77	(S)-Norcorydine	-7.6±0.00	2.17
Annonamine	-8.2±0.07	0.84	Atherospemine	-7.5±0.00	2.58
Cyclopeptides					
Annomuricatin C	-11.5±0.00	0.00			
Annomuricatin A	-10.25±0.07	0.02			

Table Ib. Ligands from *Annona muricata* and Standard drugs showing docking scores and the Inhibition Constants of the Interaction of Ligands with the Crystal structure of Sterol 14 α-demethylase (PDB ID: 5TZ1)

Ligands	Binding Affinity (ΔG), kcal/mol	Inhibition constants (K_i), μM	Ligands	Binding Affinity (ΔG), Kcal/Mol	Inhibition constants (K_i), μM
Flavonoid triglycosides					
Kaempferol-3-0-Rutinoside	-9.4±0.14	0.10	Chlorogenic acid	-8.2±0.07	0.84
Quercetin3-0-Rutinosid	-9.4±0.07	0.10	Epicatechine	-8.1±0.07	1.00
Quercetin3-O-Neohesperidoside	-9.3±0.78	0.12	Catechine	-8.0±0.00	1.09
Quercertin 3-0-Glucoside	-8.5±0.00	0.46	Kaempferol	-7.9±0.21	1.41
Quercetin	-8.2±0.85	0.77			
Megastigmanes					
Dicaffeoylquinic acid	-9.8±0.14	0.05	Caffeoylquinic acid	-8.1±0.00	0.92
4-Feruloyl-5-caffeoylquinic Acid	-9.3±0.00	0.12	Feruloylglycoside	-7.7±0.00	1.83
Dihydrokaempferol-hexoside	-8.9±0.00	0.23			
Standard Antiviral drugs					
Voriconazole (SD1)	-7.65±0.07	1.99			
Fluconazole (SD2)	-7.3±0.00	3.65			

ADMET profile predicts that a drug molecule should have good human intestinal absorption (+HIA), ability to cross the blood-brain barrier (+BBB), solubility (Log S) within the range of -1 to -5, non-inhibitors of cytochrome enzyme (P450), and toxicity in terms of Ames mutagenesis should be negative or non-Ames toxic. Also, it must exhibit non-carcinogenicity, non-inhibition of hERG, and no or low level of toxicity (Tsaioun and Kates, 2010).

Table II presents the ADMET analysis result. Out of the 131 ligands subjected to ADMET analysis, only 16 lead compounds with an inhibition constant estimated to be ≤ 1.0 were subjected to ADMET analysis across the six phytochemicals (acetogenins, alkaloids, cyclopeptides, flavonoids triglycosides, megastigmanes, and phenolics) from *Annona muricata*. The sixteen ligands are non-genotoxic and non-carcinogenic. Also, all the ligands possess type III (slightly toxic) and they could be easily converted to type IV (non-toxic) during lead optimization. The human ether-a-go-go- related gene (hERG) functions as repolarization of cardiac, blockage of this could result from some molecules present in drug or inherited mutation thereby leading to QT syndrome and eventual death (Sanguinetti and Tristanifirouzi, 2006). Fortunately, all 16 ligands were non-inhibitors of hERG. The Ames toxicity value reveals the potential of a drug molecule to cause mutation in DNA and could be a reason for excluding a drug molecule during the discovery process (Falade *et al.,* 2021). As part of the major reason for screening, all the 16 ligands passed Ames mutagenicity with negative values. All the ligands were well absorbed in the human intestine and they possess the ability to cross the blood-brain barrier and also have aqueous solubility values within the recommended range showing that the ligands possess excellent absorption and distribution properties. Similarly, all 16 ligands are non-inhibitors of microsomal enzymes which indicates good metabolism of the drug (http://lmmd.ecust.edu.cn/admetsar2/). Therefore, all 16 lead ligands have excellent ADMET properties and were subjected to further analysis for continuous validation of their potential as probable inhibitors of the receptor under study.

Drug-Likeness Analysis

The most common approach in drug discovery is to use some type of molecular descriptors linked with pattern recognition or interpolation technique, to distinguish between a

Table II. ADMET analysis of phytochemicals from *Annona muricate*

Ligands	Absorption &Distribution			Metabolism (CYP450 Inhibitors)					Extn.	Toxicity					
	BBB (+/-)	HIA (+/-)	AS (LogS)	2C19	3A4	2C9	2D6	1A2	B (+/-)	AM	AOT	EI	EC	hI	C
L1	0.91 (+)	0.99 (+)	3.09 (-)	-	-	-	-	-	-	-	III	-	-	-	-
L2	0.91 (+)	0.99 (+)	2.91 (-)	-	-	-	-	-	-	-	III	-	-	-	-
L3	0.91 (+)	0.98 (+)	2.79 (-)	-	-	-	-	-	-	-	III	-	-	-	-
L4	0.91 (+)	0.97 (+)	2.91 (-)	-	-	-	-	-	-	-	III	-	-	-	-
L5	0.91 (+)	0.99 (+)	2.91 (-)	-	-	-	-	-	-	-	III	-	-	-	-
L6	0.91 (+)	0.97 (+)	2.63 (-)	-	-	-	-	-	-	-	III	-	-	-	-
L7	0.88 (+)	0.97 (+)	2.29 (-)	-	-	-	-	-	-	-	III	-	-	-	-
L8	0.91 (+)	0.99 (+)	2.91 (-)	-	-	-	-	-	-	-	III	-	-	-	-
L9	0.89 (+)	0.99 (+)	2.29 (-)	-	-	-	-	-	-	-	III	-	-	-	-
L10	0.89 (+)	0.99 (+)	1.99 (-)	+	-	-	+	+	-	-	III	-	-	-	-
L11	0.34 (-)	0.98 (+)	1.86 (-)	-	-	-	-	-	-	-	III	-	-	-	-
L12	0.3 (-)	0.9 (+)	2.46 (-)	-	-	-	-	-	-	-	III	-	-	-	-
L13	0.77 (+)	0.76 (+)	2.36 (-)	-	-	-	-	-	-	-	III	-	-	-	-
L14	0.92 (-)	0.72 (+)	2.45 (-)	-	-	-	-	-	-	-	III	-	-	-	-
L15	0.3 (-)	0.9 (+)	2.46 (-)	-	-	-	-	-	-	-	III	-	-	-	-
L16	0.77 (-)	0.48 (-)	1.46 (-)	-	-	-	-	-	-	-	III	-	-	-	-
SD1	0.91 (-)	0.99 (+)	3.01 (-)	+	-	+	-	-	-	-	III	-	-	-	-
SD2	0.94 (+)	0.99 (+)	1.86 (-)	+	-	-	-	-	-	-	III	-	-	-	-

BBB = Blood Brain Barrier, HIA= Human Intestinal Absorption, AS= Aqueous Solubility; Extn. = Excretion, B= Biodegradation (+/-) Biodegradable (+), Non-biodegradable (-); AM= Ames mutagenesis (+/-) Acute toxicity (+), Non-Toxic (-); AOT= Acute Oral Toxicity, EC= Eye corrosion, EI=Eye Irritation; hI= Human either-a-go-go inhibition, C= Carcinogenicity; L1=Annocatacin A; L2=Arianacin; L3=Cis-annonacin-10-one; L4=Muricin E, L5=Annonacin; L6=Annopentocin A; L7=Muricin m; L8=Goniothalamicin; L9=Muricatocin C; L10= Coreximine; L11=Annomuricatacin A; L12= Chlorgenic acid; L13= Roseoside; L14= Dicaffeoylqunic acid; L15= Dihydrokaempferol-hexoside; L16= Caffeoylquinic acid; SD1= Voriconazole; SD2= Fluconazole

data set of drugs and one of the non-drugs. Drug-likeness of phytochemicals follows the pioneering "rule of five" by Lipinski (Brustle *et al.*, 2002). The following rules must be obeyed with one (1) violation at most. For a molecule to obey "the rule of five", it must exhibit molecular weight (MW) ≤ 500 Da as an oral bioavailability criterium, hydrogen bond donor (HBDs) ≤ 5, hydrogen bond acceptor (HBAs) ≤ 10, and LogP (octanol-water partition coefficient) ≤ 5. These descriptors of oral

Table III. Drug-likeness Analysis

Ligands	Molecular Formula	Lipinski's rule of five	
		Properties	**Value**
Muricin M	$C_{24}H_{42}O_7$	Molecular weight(≤500Da)	442.59
		LogP(≤5)	3.18
		H-Bond donor(≤5)	4
		H-Bond acceptor(≤10)	7
		Violation	0
Coreximine	$C_{19}H_{21}NO_4$	Molecular weight(≤500Da)	327.38
		LogP(≤5)	1.94
		H-Bond donor(≤5)	2
		H-Bond acceptor(≤10)	5
		Violation	0
Chlorogenic acid	$C_{16}H_{18}O_9$	Molecular weight(≤500Da)	354.31
		LogP(≤5)	-0.45
		H-Bond donor(≤5)	6
		H-Bond acceptor(≤10)	9
		Violation	1
Caffeoylquinic acid	$C_{16}H_{18}O_9$	Molecular weight(≤500Da)	354.31
		LogP(≤5)	-0.45
		H-Bond donor(≤5)	6
		H-Bond acceptor(≤10)	1
		Violation	1
Roseoside	$C_{19}H_{30}O_8$	Molecular weight(≤500Da)	386.44
		LogP(≤5)	-0.19
		H-Bond donor(≤5)	5
		H-Bond acceptor(≤10)	8
		Violation	0
Voriconazole	$C_{16}H1_4F_3N_5O$	Molecular weight(≤500Da)	349.32
		LogP(≤5)	1.49
		H-Bond donor(≤5)	1
		H-Bond acceptor(≤10)	8
		Violation	0
Fluconazole	$C_{13}H_{12}F2N_6O$	Molecular weight(≤500Da)	306.28
		LogP(≤5)	-0.12
		H-Bond donor(≤5)	1
		-Bond acceptor(≤10)	7
		Violation	0

bioavailability are important as they predict the permeability and absorption of such drug across a biological membrane such as an epithelium cell, partition coefficient value (log p) which is important in predicting intestinal absorption of such drug (Aucamp *et al.,* 2015).

The drug-likeness analysis of the sixteen leads showed that only five of the screened ligands and the standard drugs obeyed Lipinski's rule of five with excellent drug-like properties (Table III). Although, among the five ligands, chlorogenic acid and caffeoylquinic acid have one violation each. This indicates that the lead compounds have good oral bioavailability and permeability. So, they could be analyzed further as potential drugs.

Bioactivity Analysis

The bioactivity test is the base for therapeutic utilization and the potentially harmful effects of products prepared from plants (Coria-Téllez *et al.,* 2016). The Ligand efficiency (LE), Fit Quality (FQ), and Ligand Efficiency-dependence lipophilicity (LELP) of the five (5) excellent lead compounds are presented in Table IV. Inhibition constant values of these compounds range from 0.46 to 1.3 μM, this showed that all of these

Table IV. Bioactivity properties

Ligands	AutoDock Vina docking score (kcal/mol)	Ki (μM)	miLOG P	L.E (kcal/mol/ heavy atom)	L.E-Scale	F.Q	LELP
L1	-8.5	0.46	1.66	0.35	0.44	0.81	4.74
L2	-8.5	0.46	-3.50	0.31	0.41	0.76	-11.29
L3	-8.2	0.84	1.13	0.33	0.43	0.77	3.42
L4	-8.1	0.92	-0.45	0.32	0.43	0.74	-1.41
L5	-7.9	1.3	3.18	0.25	0.37	0.68	12.72
SD1	-7.65	1.99	1.49	0.31	0.43	0.72	4.81
SD2	-7.3	3.65	-0.12	0.33	0.46	0.72	-0.36

L1= Coreximine; L2= Roseoside; L3= Chlorogenic; L4= Caffeoylquinic acid; L5 = Muricin M; SD1= Voriconazole; SD2= Fluconazole

compounds are within the acceptable range of 0 to 1.0 μM, except muricin M with a slightly higher value of 1.3 μM (Table IV). The heavy atoms in the structure of the ligands were used to calculate ligand efficiency (LE), with a recommended value ≥ 0.3. Fit Quality (FQ) was evaluated with a recommended value ≥ 0.8, and Ligand Efficiency-dependence lipophilicity (LELP) was also determined with the expected recommended value in the range of -10 to 10 using equations 1 to 4. Notably, all five ligands and the two standard drugs have excellent bioactivity properties in the right proportion as recommended, it is important to note that none of the ligands fails the bioactivity test.

Ligand Efficiency (LE) = −B.E ÷ Heavy atoms (H.A) ……(1)

LE scale = $0.873e^{-0.026\times H.A}-0.064$……(2)

FQ = LE ÷ LE scale……(3)

LELP = LogP ÷ LE……(4)

Binding Mode and Molecular Interactions of the Selected Hits and Standards

The identification of the binding site and evaluation of the binding interaction of the ligands in the active pocket of the target receptor is important in the drug discovery process. This helps in ligand modification during the lead optimization stage of drug discovery (Falade *et al.,* 2021). The molecular docking study predicted the residues at the interacting site of the proteins as well as their corresponding alignments (Adeoye *et al.,* 2019). Table V and VI show the binding affinities and molecular interactions of selected lead compounds respectively. muricin M forms a conventional hydrogen bond with Met508, Tyr505, Ser507, and His377, pi-alkyl interaction with Phe380, Leu121, Pro230, Val234, Tyr132, and Leu88, unfavourable donor bond with Ser378 (Table V and VI). Upon examining the active site of the target receptor (5TZ1), it was revealed that its binding pocket (active site) was located in the heme loop and helix loop. All the other residues of muricin N reported in Table VI were found at the active site of the target receptor (sterol 14α-demethylase , PDB ID 5TZ1) except Leu88 and Val234 that was mentioned earlier in the structural and active site analysis of sterol 14α-demethylase (PDB ID: 5TZ1). This implies that muricin M shares the same pocket and interacts effectively with the active site of the target receptor, hence it could be a potent inhibitor of the receptor.

Similarly, chlorogenic acid, roseoside, and caffeoylquinic acid showed strong interactions with 5TZ1 when compared with the standards (Table V and VI). Chlorogenic acid formed a conventional hydrogen bond with Pro230, Gly65, Tyr505, Met508, His377, Ser378, hydrogen carbon bond interactions with Ser507, pi-sulphur bond interactions with Met508, and unfavourable pi-bond interactions with His377 (Table V and VI). Roseoside formed a conventional hydrogen bond with Ser378, Met508, Pro230, Ser507, His377, Phe58, and pi-alkyl interactions with Tyr64, Phe380, Phe233, Leu87, Leu88, Val234, while Caffeoylquinic acid formed a conventional hydrogen bond with Ile304, His468, Arg381, Ile471, Gly308, and alkyl interactions with Lys143, Ile471, Ile131, Cys470, carbon-hydrogen interactions with Gly464, and unfavourable donor interactions with Arg381. The excellent binding affinities of these ligands influence the molecular interactions (Tables V and VI). Therefore, chlorogenic acid, roseoside, and caffeoylquinic acid were found to have most of their residues at the active site of sterol 14α-demethylase better than the two standard drugs.

Table V. Binding mode and molecular interactions of the selected hits against 5TZ1

Ligands	Binding pocket	Interaction
L1-Muricin M	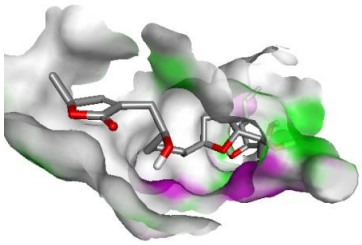	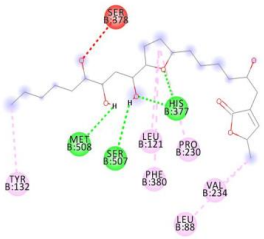
L2-Chlorogenic Acid	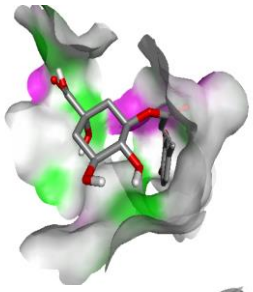	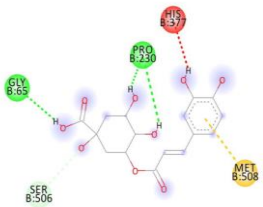
L3-Roseoside	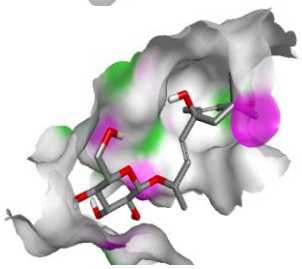	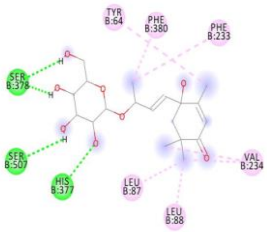
L4-Caffeolyquinic acid	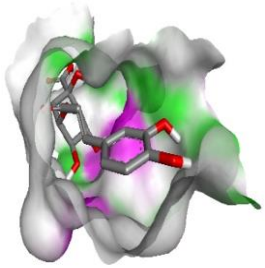	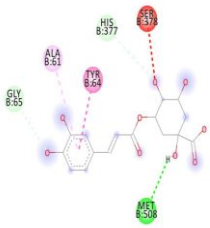
SD1 Voriconazole	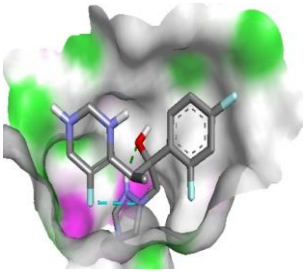	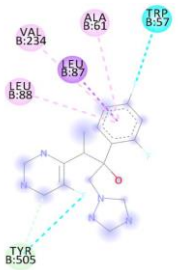
SD2- Fluconazole	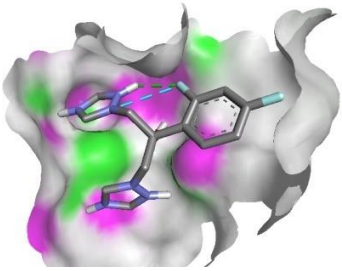	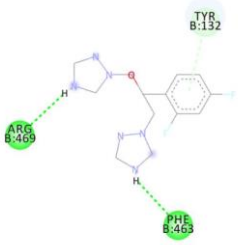

Table VI. Docking scores, binding sites and inhibition constants of the selected hit compounds and standards with sterol 14 α-demethylase

Ligands	Binding Affinity (ΔG), kcal/mol	Receptor amino acids forming H-bond with ligands (H-bond Distance, Å)	Electrostatic/Hydrophobic Interactions	Inhibition constants (Ki), μM
Muricin M	-7.9±0.00	Met508 (2.8 Å), Met508 (3.2 Å) Tyr505(3.0 Å) Ser507(3.1 Å) His377 (2.9 Å)	Phe380, Ser378, Leu121, Pro230, Val234, Tyr132, Leu88	1.30
Chlorogenic Acid	-8.2±0.07	Pro230(2.8 Å) Gly65(2.9 Å) Pro230(3.5 Å) Tyr505(2.9 Å) Tyr505(3.0 Å) Met508(2.9 Å) His377(2.7 Å) Ser378(2.2 Å) Ser378(2.8 Å)	Ser506, Met508, His377	0.84
Roseoside	-8.5±0.64	Ser378(2.8 Å) Ser378(3.2 Å) Met508(3.0 Å) Pro230(3.0 Å) Ser507(3.0 Å) His377(2.1 Å) Phe58(3.2 Å)	Tyr64, Phe380, Phe233, Leu87, Leu88, Val234	0.46
Caffeoylquinic acid	-8.1±0.00	Ser378(1.9 Å) His377(2.4 Å) Tyr505(3.1 Å) Met508(2.8 Å) Met508(2.8 Å) Ser378(3.0 Å)	Ala61, Tyr64, Ser378, His377, Gly65	0.92
Voriconazole	-7.65±0.07	Tyr132(2.2Å) Arg469(2.3 Å) Phe463(2.3 Å) Tyr132(2.4 Å)	Val234, Ala61, Leu87, Leu88, Trp57, Tyr505	1.99
Fluconazole	-7.3±0.00	Phe463 Arg469	Tyr132	3.65

CONCLUSION

This research work evaluated one-hundred and thirty-one (131) ligands from *Annona muricata* (sour sop) against sterol 14α-demethylase using an in-silico approach (structure-based drug design). All these ligands were screened with the PyRx visual screening tool, ADMET SAR-2, Molinspiration web server, and many others. CASTp web tool was also used to validate their active site. The results obtained exceptionally favour muricin M (-7.9 kcal/mol), chlorogenic acid (-8.2 kcal/mol), roseoside (-8.5 kcal/mol), and caffeoylquinic acid (-8.1 kcal/mol) as probable inhibitors of sterol 14α-demethylase due to their outstanding binding energies, ADMET profile, drug-likeness, Bioactivity, favourable binding mode and molecular interactions with the target receptor (5TZ1). muricin M, chlorogenic acid, roseoside, and caffeoylquinic acid had shown favourable properties as potential inhibitors of 5TZ1 than voriconazole and fluconazole which have been in use for decades as first-line drugs for treating fungal infections (Hargrove *et al*., 2017). Since computational drug design is widely accepted in the world of modern drug design and development, the aforementioned ligands could be developed further and subjected to both pre-clinical studies and clinical trials toward the

development of a new anti-fungal drug. This research work has identified muricin M, chlorogenic acid, roseoside, and caffeoylquinic acid as potential inhibitors of sterol 14α-demethylase (PDB: 5TZ1). It is hereby recommended that structural modification of these ligands could be carried out via a lead optimization process to improve their potency, efficacy, and pharmacokinetics, and reduce their toxicity in human trials toward the development of new anti-fungal therapeutic agents.

ACKNOWLEDGEMENT

The authors acknowledge the members of the Computational and Biophysical Chemistry Research Group at the Department of Pure and Applied Chemistry, Ladoke Akintola University of Technology (LAUTECH), Ogbomoso, Oyo State, Nigeria.

REFERENCES

Aanouz, I., Belhassan, A., El Khatabi, K., Lakhlifi, T., El Idrissi, M. & Bouachrine, M., 2020, 'Moroccan Medicinal Plants as Inhibitors of COVID-19: Computational Investigations', *J. Biomol. Struct. Dyn*., 39 (1), 1-12.

Abdul-Hammed, M., Adedotun, I.O, Mufutau, K., Towolawi, B., Afolabi, T. & Irabor, C., 2022, 'Antibreast cancer activities of phytochemicals from *Annona muricata* using computer-aided drug design (CADD) approach', *Phys. Sci. Rev.*

Abdul-Hammed, M., Adedotun, I.O, Falade, V.A, Adepoju, A.J, Olasupo, S.B. & Akinboade, M.W., 2021, 'Target-based drug discovery, ADMET profiling and bioactivity studies of antibiotics as potential inhibitors of SARS-CoV-2 main protease (M^{pro})', *Virus disease*. 1-15.

Adeoye, A.O., Olanlokun, J.O., Tijani, H., Lawal, S.O., Babarinde, C.O., Akinwole, M.T. & Bewaji, C. O., 2019, 'Molecular docking analysis of apigenin and quercetin from ethyl acetate fraction of Adansonia digitata with malaria-associated calcium transport protein: An In-silico approach'. *Heliyon*, 5 (9), e02248. 1

Agu, K.C. & Okolie, P. N., 2017. 'Proximate composition, phytochemical analysis and in vitro antioxidant potentials of extracts of *Annona muricata* (Soursop)', *Food Sci. Nutr.,* 5, 1029-1036.

Al Aboody, M.S. & Mickymaray, S., 2020, 'Anti-Fungal Efficacy and Mechanisms of Flavonoids' *Department of Biology, College of Science, Al-Zulfi, Majmaah University, Riyadh Region, Majmaah 11952, Saudi Arabia,* 9 (45), 1-4.

Aucamp, M., Odendaal, R., Liebenberg, W. & Hamman, J., 2015, 'Amorphous azithromycin with improved aqueous solubility and intestinal membrane permeability', *Drug Dev. Ind. Pharm*., 41 (7), 1100-1108.

Bongomin, F., Gago, S., Oladele, R.O. & Denning, D.W., 2017, 'Global and Multi-National Prevalence of Fungal Diseases-Estimate Precision', *J. fungal*, 3 (4), 57 1-29.

Brustle, M., Beck, B., Schindler, T., King, W., Mitchell, T. & Clark, T., 2002, 'Descriptors, Physical Properties, and Drug-Likeness', *J. Med. Chem*., 45, (16), 3345-3355.

Coria-Téllez, A.V., Montalvo-Go´nzalez, E., Yahia, E. M. & Obledo-Vázquez, E. N., 2016, '*Annona muricata*: A comprehensive review on its traditional medicinal uses, phytochemicals, pharmacological activities, mechanisms of action and toxicity', *Arab. J. Chem.,* 11, 662–691.

Daina, A., Michielin, O. & Zoete, V., 2017, 'SwissADME: a free web tool to evaluate pharmacokinetics, drug-likeness and medicinal chemistry friendliness of small molecules', *Sci. Rep*., 7, 1-13

Dallakyan, S. & Olson, A.J., 2015, 'Small Molecule Library Screening by Docking with PyRx', *Research gate*, 1-12

Dong, Y., Liu, M., Wang, J., Ding, Z. & Sun, B., 2019, 'Construction of antifungal dual-target (SE, CYP51) Pharmacophore models and the discovery of novel antifungal inhibitors', *The Royal Society of Chemistry*, 9, 26302-26314.

El-Hachem, N., Haibe-Kains, B., Khalil, A., Kobeissy, F. H. & Nemer, G., 2017, 'AutoDock and AutoDock Tools for Protein-Ligand Docking: Beta-Site Amyloid Precursor Protein Cleaving Enzyme 1(BACE1) as a Case Study', *Springer Science Business Media,* 1598, 1-13.

Falade,V.A., Adelusi,T.I., Adedotun, I.O., Abdul-Hammed, M., Lawal, T.A., Agboluaje, S.A., 2021, 'In-silico investigation of saponins and tannins as potential inhibitors of SARS-CoV-2 main protease (M^{pro})', *In Silico Pharmacol*., 9 (1), 9.

Ferreira, T.M., Costa A.A., Vicenta, R. & Varum, H., 2015, 'A simplified four-branch model for the analytical study of the out-of-plane performance of regular stone URM walls' *Eng. Struct.,* 83, 140-153.

Hargrove, T. Y., Friggeri, L., Wawrzak,Z., Qi, A., Hoekstra, W. J., Schotzinger, R. J., York, J. D., Guengerich, F. P. & Lepesheva, G. I., 2017, 'Structural analyses of Candida albicans sterol 14α-demethylase complexed with Azole drugs address the molecular basis of

azole-mediated inhibition of fungal sterol biosynthesis', The *American Society for Biochemistry and Molecular Biology*, 292 (16) 6728-6743.

Kohler, J.R., Casadevall, A. & Perfect, J., 2015, 'The Spectrum of Fungi That Infects Humans, 'C*old Spring Harb. perspect. med*., 1-14.

Moghadamtousi, S.Z., Fadaeinasab, M., Nikzad, S., Mohan, G., Ali, H.M. & Habsah Abdul Kadir., 2015, '*Annona muricata* (Annonaceae): A Review of Its Traditional Uses, Isolated Acetogenins and Biological Activities', *Int. J. Mol. Sci*., 16, 15625-15658.

Sanguinetti, M.C. & Tristani-firouzi M., 2006, 'hERG potassium channels and cardiac arrhythmia,' *Nature*, 440, 463-469.

Sheng, C., Miao, Z., Ji, H., Yao J., Wang, W., Che, X., Dong, G. Lu, J., Guo, W. & Zhang W., 2009, 'Three-dimensional model of lanosterol 14α-demethylase from *cryptococcus neoformans*: Active-site characterization and insights into Azole binding, 'Antimicrob. Agents Chemother*.,* 53 (8), 3487-3495.

Tian, W., Chen, C., Lei, X., Zhao J. & Liang, J., 2018, 'CASTp 3.0: computed atlas of surface topography of proteins, '*Nucleic Acids Res.,* 46, 363-368.

Tsaioun, K. & Kates, S.A., 2010, 'ADMET for medicinal chemists: A practical guide', *John Wiley and Sons, Singapore*, 145-200.

Tudela, J.L.R. & Denning, D.W., 2017, 'Recovery from serious fungal infections should be realizable for everyone', *Global Action Fund for Fungal Infections, 1211 Geneva 1, Switzerland (JLRT, DWD) and The National Aspergillosis Centre, University Hospital of South Manchester, The University of Manchester, Manchester Academic Health Science Centre, Manchester, UK* (DWD):1-3.